

3. ANALYTICAL METHODS

3.1. Analytical methods for Doxorubicin (DOX):

3.1.1. UV-Visible spectrophotometric method:

3.1.1.1. Materials:

Doxorubicin hydrochloride was obtained as a gift sample from Sun Pharmaceuticals Ltd., India. Potassium dihydrogen phosphate, disodium hydrogen phosphate and sodium chloride were of analytical grade and purchased from Loba Chemie, India. The water used in the study was double distilled.

3.1.1.2. Equipments:

Digital Analytical Weighing Balance (Shimadzu, Switzerland)

pH Meter (Labindia, India)

UV-Visible Spectrophotometer 1800 (Shimadzu, Japan)

3.1.1.3. Estimation of DOX:

➤ **Reagent preparation (Phosphate buffer pH 7.4):**

2.38 g of disodium hydrogen phosphate, 0.19 g potassium dihydrogen phosphate and 8.0 g of sodium chloride were dissolved in sufficient water to produce 1000 ml and then the pH was adjusted to 7.4.

➤ **Preparation of stock solution:**

Stock solution was prepared by dissolving 10 mg of drug in 100ml of phosphate buffer (pH-7.4) to get concentration of 100 µg/ml.

➤ **Procedure for calibration curve:**

Appropriate aliquots of stock solution of DOX (0.5 to 2.5ml) were transferred to 10 ml volumetric flasks and made up to the mark with phosphate buffer (pH 7.4) to get final concentration of drug in range of 5-25 µg/mL. Scanning was performed in range of 800-200 nm to determine the λ_{\max} using phosphate buffer (pH 7.4) as blank. The absorbance maximum (λ_{\max}) was found to be 480 nm, which is the typical absorption for DOX. The absorbance as a function of concentration for all prepared solutions was recorded against phosphate buffer (pH 7.4).^{1,2} The procedure was repeated in triplicate and the observations were recorded. Mean value of the absorbance (n=3) along with standard deviation (S.D.) and other parameters of developed UV spectrophotometric method are

recorded in table 3.1. The regression of the plot using the method of least squares was made to evaluate the intercept, slope and coefficient of determination (r^2) as shown in figure 3.1. The high value of r^2 (near 1) and negligible value of intercept confirmed the linearity of the calibration plot.

Table 3.1: Calibration curve of DOX in PBS (pH 7.4) by UV-Visible spectrophotometer.

Sr. No.	Concentration ($\mu\text{g/ml}$)	Mean Absorbance	\pm S.D. (n=3)
1	5	0.10042	0.00120
2	10	0.18306	0.00216
3	15	0.26773	0.00326
4	20	0.35831	0.00428
5	25	0.44446	0.00546

λ_{max} (nm)	Conc. Range ($\mu\text{g/ml}$)	Mean S.D.	LOD	LOQ	Regression Equation	Regression Coefficient
480.7	5 - 25	0.00325	0.209	0.697	$y=0.0173x+0.0118$	0.999

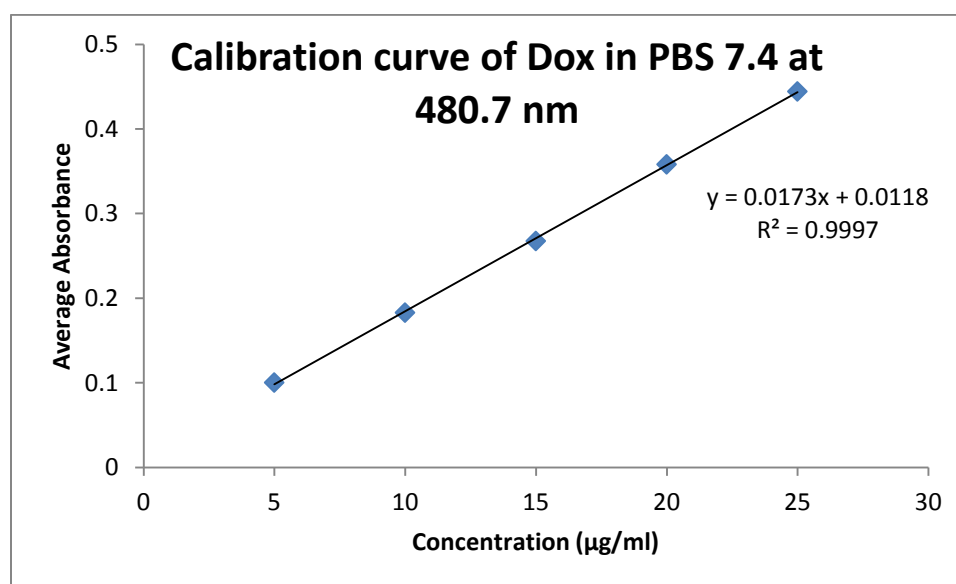


Figure 3.1: Standard calibration curve of DOX in PBS 7.4 by UV Visible spectroscopy.

3.1.2. Interference study:

The interference study of doxorubicin hydrochloride with synthesized mesoporous silica nanoparticles and copper oxide loaded mesoporous silica nanoparticles was done by UV visible spectrophotometry.

Solutions of 25 $\mu\text{g/ml}$ for each sample (DOX, MSN, and CuO-MSN) were prepared from the stock solution (100 $\mu\text{g/ml}$ which were prepared by adding 10 mg of said sample to 100 ml of PBS 7.4) of the respective samples and the absorption spectra was recorded from 800-200 nm range keeping PBS 7.4 as a blank.

As shown in the figure 3.2, plain MSNs showed no significant interference but CuO-MSN showed significant absorbance throughout the absorption window and was found to interfere with the absorbance of the DOX at 480.7 nm. Hence, UV-Visible spectrophotometry method was not found suitable for the analysis of DOX when CuO-MSNs were used as a carrier.

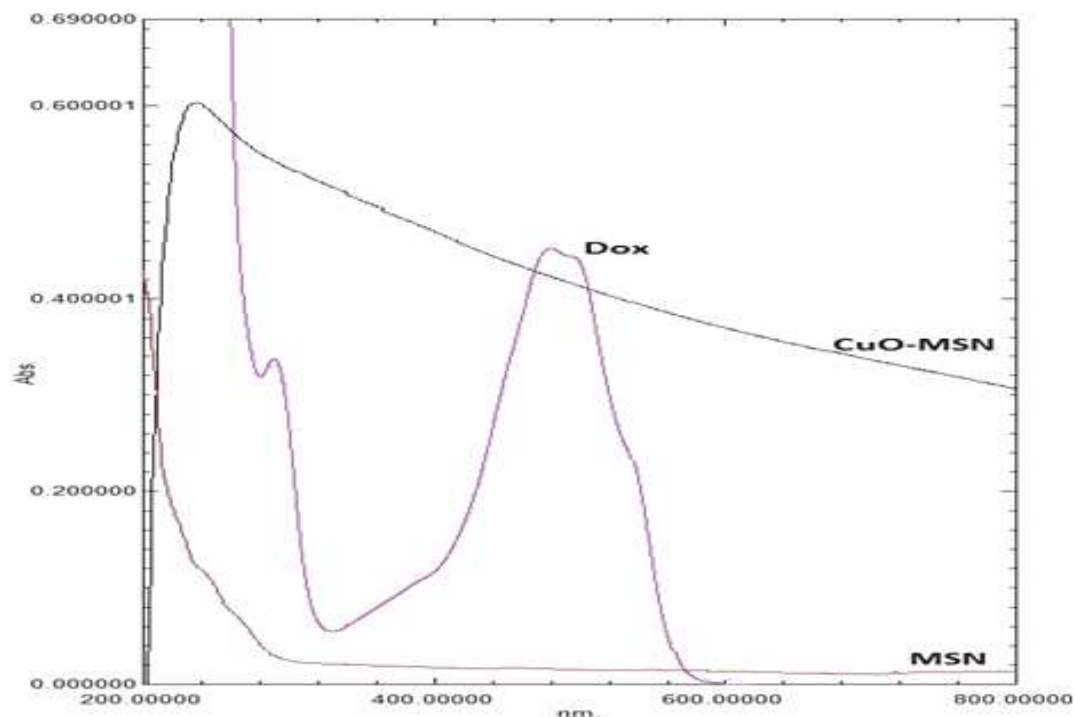


Figure 3.2: UV visible spectra of DOX, MSN and CuO-MSN in PBS 7.4 for interference studies.

3.1.3. Spectrofluorimetric Method:

Spectrofluorimetric analytical method was developed for DOX as UV-Visible method was found inappropriate for determination of DOX in the presence of developed CuO-MSN. DOX is reported to produce emission spectra from 525 to 625 nm, when excited at 480 nm.³

3.1.3.1. Materials:

Doxorubicin hydrochloride was obtained as a gift sample from Sun Pharmaceuticals Ltd., India. Potassium dihydrogen phosphate, disodium hydrogen phosphate and sodium chloride were of analytical grade and purchased from Loba Chemie, India. The water used in the study was double distilled.

3.1.3.2. Equipments:

Digital Analytical Weighing Balance (Shimadzu, Switzerland)

pH Meter (Labindia, India)

RF-5301 PC Spectrofluorophometer (Shimadzu, Germany)

3.1.3.3. Estimation of DOX in PBS (pH 7.4):

➤ **Reagent preparation (PBS pH 7.4):**

2.38 g of disodium hydrogen phosphate, 0.19 g potassium dihydrogen phosphate and 8.0 g of sodium chloride were dissolved in sufficient water to produce 1000 ml and the pH was adjusted to 7.4.

➤ **Preparation of stock solution:**

Stock solution was prepared by dissolving 10 mg of drug in 100ml of phosphate buffer (pH-7.4) to get concentration of 100 µg/ml.

➤ **Procedure for calibration curve:**

First the stock solution was scanned over the range of 220 to 700 nm to determine the excitation maxima. The excitation wavelength of DOX was found 480 nm which was matched with the previously reported excitation wavelength.

Appropriate aliquots of stock solution of DOX (50-250 µl) were transferred to a 10 ml volumetric flask and made up to the mark with phosphate buffer (pH 7.4) to get final concentration of drug in range of 0.5-2.5 µg/mL. Scanning was performed in range of 220-700 nm to determine the emission wavelength of the solutions when excited at 480 nm. The emission peak was found at 556 nm, which is the typical emission for DOX.

The emission as a function of concentration for all prepared solutions was recorded. The excitation and emission slit width were both set to 10 nm.⁴ Mean value of the intensity (n=3) along with standard deviation (S.D.) and other parameters of developed spectrofluorimetric method are recorded in table 3.2. The regression of the plot using the method of least squares was made to evaluate the intercept, slope and coefficient of determination (r^2) as shown in figure 3.3. The high value of r^2 (near 1) and negligible value of intercept confirmed the linearity of the calibration plot.

Table 3.2: Calibration curve of DOX in PBS (pH 7.4) by fluorescence spectroscopy.

Sr. No.	Concentration ($\mu\text{g/ml}$)	Fluorescence Intensity	\pm S.D. (n=3)
1	0.5	59.534	0.714
2	1.0	118.745	1.445
3	1.5	169.937	2.039
4	2.0	221.25	2.680
5	2.5	281.527	3.378

Excitation (nm)	Emission (nm)	Conc. Range ($\mu\text{g/ml}$)	Mean S.D.	LOD	LOQ	Regression Equation	Regression Coefficient
480	556	0.5 - 2.5	2.046	0.0196	0.0653	$y=109.3x+6.2513$	0.999

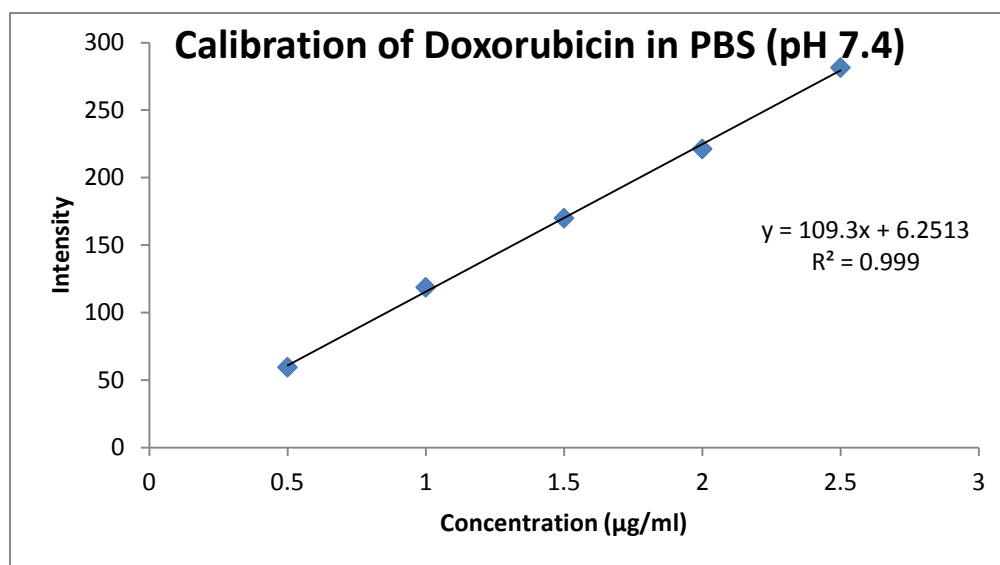


Figure 3.3: Standard calibration curve of DOX in PBS 7.4 by fluorescence spectroscopy.

3.1.3.4. Estimation of DOX in phosphate buffer (pH 5.5):**➤ Reagent preparation:**

Solution I: 13.61 g of potassium dihydrogen phosphate was dissolved in sufficient water to produce 1000 ml.

Solution II: 35.81 g of disodium hydrogen phosphate was dissolved in sufficient water to produce 1000 ml.

Then 96.4 ml of solution I was mixed with 3.6 ml of solution II.

➤ Preparation of stock solution:

Stock solution was prepared by dissolving 10 mg of drug in 100ml of phosphate buffer (pH-5.5) to get concentration of 100 µg/ml.

➤ Procedure for calibration curve:

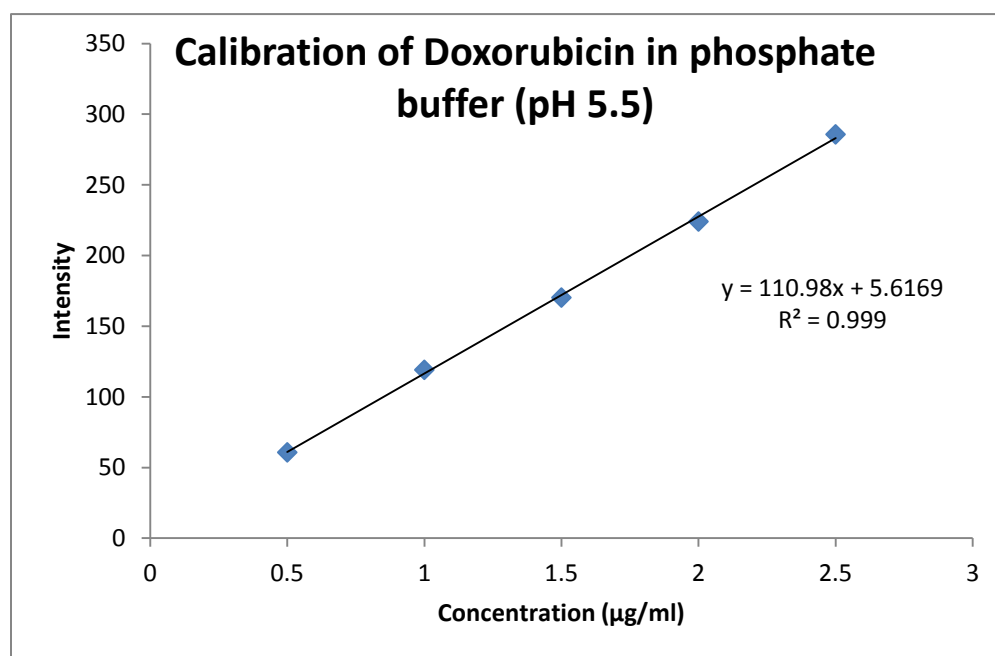
First the stock solution was scanned over the range of 220 to 700 nm to identify the excitation maxima. The excitation wavelength of DOX was found 480 nm which matched with the previously reported excitation wavelength.

Appropriate aliquots of stock solution of DOX (50-250 µl) were transferred to 10 ml volumetric flasks and made up to the mark with phosphate buffer (pH 7.4) to get final concentration of drug in range of 0.5-2.5 µg/mL. Scanning was performed in range of 220-700 nm to determine the emission maximum of the solutions when excited at 480 nm. The emission peak was found at 556 nm, which is the typical emission for DOX. The emission as a function of concentration for all prepared solutions was recorded by exciting them at 480 nm. The excitation and emission slit width were both set to 10 nm.⁴ The procedure was repeated in triplicate and the observations were recorded. Mean value of the intensity (n=3) along with standard deviation (S.D.) and other parameters of developed spectrofluorimetric method are recorded in table 3.3. The regression of the plot using the method of least squares was made to evaluate the intercept, slope and coefficient of determination (r^2) as shown in figure 3.4. The high value of r^2 (near 1) and negligible value of intercept confirmed the linearity of the calibration plot.

Table 3.3: Calibration curve of DOX in phosphate buffer (pH 5.5) by fluorescence spectroscopy.

Sr. No.	Concentration ($\mu\text{g/ml}$)	Fluorescence Intensity	\pm S.D. (n=3)
1	0.5	60.842	0.730
2	1.0	119.245	1.431
3	1.5	170.361	2.148
4	2.0	224.166	2.706
5	2.5	285.837	3.43

Excitation (nm)	Emission (nm)	Conc. Range ($\mu\text{g/ml}$)	Mean S.D.	LOD	LOQ	Regression Equation	Regression Coefficient
480	556	0.5 - 2.5	2.089	0.0197	0.0658	$y=110.98x+5.617$	0.999

**Figure 3.4:** Standard calibration curve of DOX in phosphate buffer (pH 5.5) by fluorescence spectroscopy.

3.1.3.5. Interference study:

The interference of DOX with synthesized mesoporous silica nanoparticles and copper oxide loaded mesoporous silica nanoparticles as well as with chitosan-folate conjugate (CH-FA) was checked for fluorescence spectroscopy.

Solutions of 2.5 µg/ml for each sample (DOX, MSN, CuO-MSN and CH-FA) were prepared from the stock solution (100 µg/ml which was prepared by adding 10 mg of said sample to 100 ml of PBS 7.4) of the respective samples in PBS (pH 7.4) and the spectra were recorded from 220-700 nm range keeping 480nm as the excitation wavelength for DOX. None of the samples showed any emission at 556 nm (emission wavelength of DOX) other than DOX. Hence, the spectrum for 2.5 µg/ml DOX solution, 1:1 mixture of DOX: MSN (2.5 µg/ml : 2.5 µg/ml), 1:1 mixture of DOX:CuO-MSN (2.5 µg/ml : 2.5 µg/ml), 1:1 mixture of DOX:MSN:CH-FA (2.5 µg/ml : 2.5 µg/ml : 2.5 µg/ml) and 1:1 mixture of DOX:CuO-MSN:CH-FA (2.5 µg/ml : 2.5 µg/ml : 2.5 µg/ml) was recorded at a fixed excitation wavelength of 480 nm and any changes in the emission intensity at 556 nm was observed.

Table 3.4: Interference study data of different compounds by fluorescence spectroscopy.

Sr. No.	Name of compound	Fluorescence Intensity	± S.D. (n=3)
1	DOX	281.527	3.378
2	DOX + MSN	280.634	3.216
3	DOX + CuO-MSN	282.271	3.410
4	DOX + MSN + CH-FA	283.167	3.242
5	DOX + CuO-MSN + CH-FA	283.836	3.351

From the Table 3.4, it can be seen that, no major difference in the emission intensity of DOX was observed when DOX solution alone or in combination with nanoparticles as well as polymer-ligand conjugate was excited at 480 nm. Hence, it can be said that neither nanoparticles (MSN & CuO-MSN) nor polymer-ligand conjugate (CH-FA) interfered with the analysis of DOX when analysis was performed using fluorescence spectroscopy.

3.2. Analytical methods for metal content determination:

3.2.1. Atomic Absorption spectroscopy method:

In atomic absorption spectroscopy, the amount of light which is absorbed as the light passes through a cloud of atoms is of interest. As the number of atoms in the light path increases, the amount of light absorbed increases in a predictable way. By measuring the amount of light absorbed, a quantitative determination of the amount of analyte element present can be made. The use of special light sources and careful selection of wavelength allow the specific quantitative determination of individual elements in the presence of others.⁵

The atomic absorption method of analysis as first described by Walsh et al.^{6,7} has been found to be extremely suitable for the rapid determination of magnesium⁸, zinc⁹, iron, manganese¹⁰ and copper¹¹.

3.2.1.1. Materials:

Standard $\text{CuCl}_2 \cdot 2\text{H}_2\text{O}$ solution was purchased from Sigma Aldrich, India. The water used in the study was double distilled.

3.2.1.2. Equipments:

Atomic Absorption Spectrometer AAnalyst 200 (Perkin Elmer, USA)

3.2.1.3. Estimation of copper content:

➤ **Procedure for calibration curve:**

The standard $\text{CuCl}_2 \cdot 2\text{H}_2\text{O}$ solution (1000 ppm) was diluted to 10 ml by transferring 1 ml into 10 ml volumetric flask by double distilled water (DDW) to make a stock solution of 100 $\mu\text{g}/\text{mL}$ solution. Appropriate aliquots of stock solution of $\text{CuCl}_2 \cdot 2\text{H}_2\text{O}$ (0.1 to 0.5ml) were transferred to 10 ml volumetric flasks and made up to the mark with DDW to get final concentration of drug in range of 1-5 $\mu\text{g}/\text{mL}$. The respective solutions were sprayed into a flame, and the absorption of light by the copper atoms in the flame was determined. The procedure was repeated in triplicate and the observations were recorded. Mean value of the absorbance ($n=3$) along with standard deviation (S.D.) and

other parameters of performed AAS method are recorded in table 3.5. The regression of the plot using the method of least squares was made to evaluate the intercept, slope and coefficient of determination (r^2) as shown in figure 3.5. The high value of r^2 (near 1) and negligible value of intercept confirmed the linearity of the calibration plot.

Table 3.5: Calibration curve of CuCl_2 in DDW by Atomic Absorption Spectroscopy.

Sr. No.	Concentration ($\mu\text{g/ml}$)	Mean Absorbance	\pm S.D. (n=3)
1	1	0.186	0.0011
2	2	0.371	0.0006
3	3	0.525	0.0018
4	4	0.674	0.0009
5	5	0.824	0.0014

Conc. Range ($\mu\text{g/ml}$)	Mean S.D.	LOD	LOQ	Regression Equation	Regression Coefficient
1 - 5	0.00116	0.02089	0.06966	$y=0.1579x+0.0423$	0.998

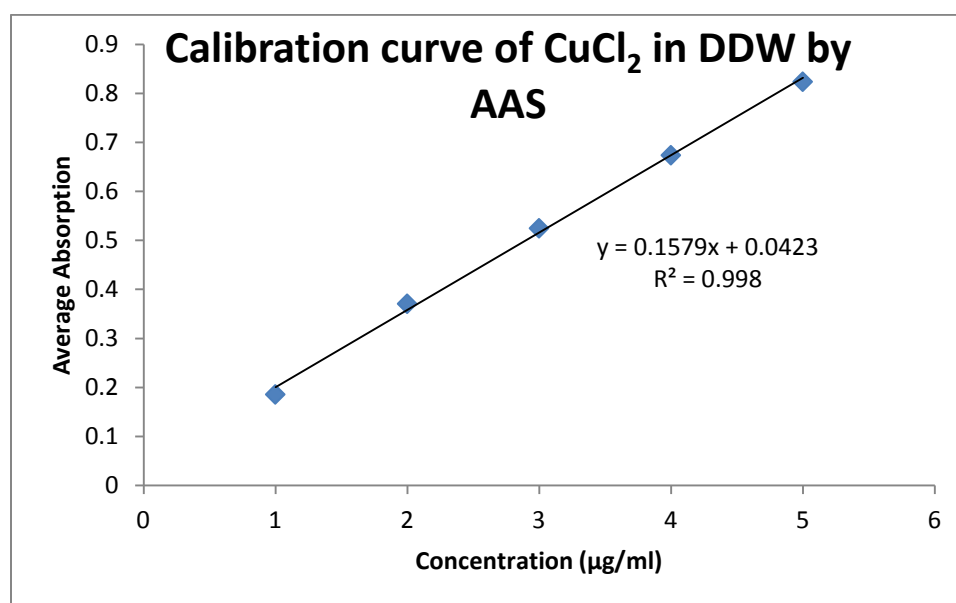


Figure 3.5: Standard calibration curve of CuCl_2 in DDW by Atomic Absorption Spectroscopy.

3.2.1.4. Estimation of zinc content:

➤ Procedure for calibration curve:

The procedure for preparation of calibration curve to determine zinc concentration was quite similar to procedure mention above in 3.2.1.3, except the use of zinc chloride (ZnCl_2) instead of copper chloride. Mean value of the absorbance ($n=3$) along with standard deviation (S.D.) and other parameters of performed AAS method are recorded in table 3.6. The regression of the plot using the method of least squares was made to evaluate the intercept, slope and coefficient of determination (r^2) as shown in figure 3.6.

Table 3.6: Calibration curve of ZnCl_2 in DDW by Atomic Absorption Spectroscopy.

Sr. No.	Concentration ($\mu\text{g/ml}$)	Mean Absorbance	\pm S.D. (n=3)
1	1	0.371	0.0049
2	2	0.638	0.0042
3	3	0.85	0.0037
4	4	1.141	0.0054
5	5	1.4	0.0048

Conc. Range ($\mu\text{g/ml}$)	Mean S.D.	LOD	LOQ	Regression Equation	Regression Coefficient
1 - 5	0.0046	0.0574	0.1914	$y=0.256x+0.1118$	0.998

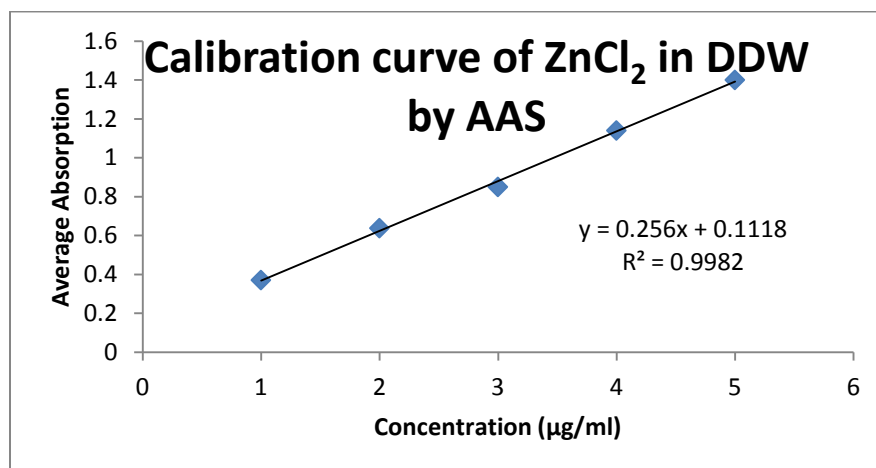


Figure 3.6: Standard calibration curve of ZnCl_2 in DDW by Atomic Absorption Spectroscopy.

3.3. Estimation of surface conjugated amino groups (Ninhydrin test):

With a view to quantify the surface density of accessible primary amines functionalized on MSN-NH₂ particles, we employed a simple, fast and relatively harmless ninhydrin-based method. Ninhydrin (2, 2-dihydroxyindane-1, 3-Dione) destroys each primary amine to form a deep purple chromogen referred to as Ruhemann's Purple, which has a maximum absorption at about 580 nm. The standard curve for the determination was made by using 3-aminopropyltriethoxysilane (APTES) as a standard material.^{12,13,14}

3.3.1. UV-Visible spectrophotometric method:

3.3.1.1. Materials:

APTES was purchased from Sigma Aldrich, India. Ninhydrin was purchased from Loba Chemie, India. Methanol AR was purchased from Rankem, India.

3.3.1.2. Equipments:

Digital Analytical Weighing Balance (Shimadzu, SCS, Switzerland)

UV-Visible Spectrophotometer 1800 (Shimadzu, Japan)

3.3.1.3. Estimation of amino groups:

➤ **Preparation of stock solution:**

Stock solution was prepared by diluting 0.1 ml of APTES in 10ml of methanol to get concentration of 10 µg/ml.

➤ **Procedure for calibration curve:**

Appropriate aliquots of stock solution of APTES (0.1 to 0.5ml) were transferred to 10 ml vials. To this, 1 ml of ninhydrin solution (7 mg/ml in methanol) was added and made up to 10ml with methanol to get final concentration of APTES in range of 100-500 µg/ml of APTES. Subsequently, the vials were capped to avoid the loss of solvent and then transferred to a boiling water bath. After 5 minutes, the vials were taken out and cooled to room temperature. Scanning was performed in range of 800-400 nm to determine the λ_{max} using methanol as blank. The absorbance maximum (λ_{max}) was found to be 581 nm.¹³ The absorbance as a function of concentration for all prepared solutions was recorded against methanol. The procedure was repeated in triplicate and the observations were recorded. Mean value of the absorbance (n=3) along with standard deviation (S.D.) and other parameters of performed UV spectrophotometric method are recorded in table 3.7. The regression of the plot using the method of least squares was

made to evaluate the intercept, slope and coefficient of determination (r^2) as shown in figure 3.7. The high value of r^2 (near 1) and negligible value of intercept confirmed the linearity of the calibration plot.

Table 3.7: Calibration curve of APTES in methanol by UV-Visible spectrophotometer.

Sr. No.	Concentration (nl/ml)	Mean Absorbance	\pm S.D. (n=3)
1	100	0.086	0.0010
2	200	0.316	0.0026
3	300	0.599	0.0022
4	400	0.861	0.0037
5	500	1.082	0.0041

λ_{\max} (nm)	Conc. Range (nl/ml)	Mean S.D.	LOD	LOQ	Regression Equation	Regression Coefficient
581	100 - 500	0.00272	0.588	1.960	$y=0.0051x-0.1723$	0.998

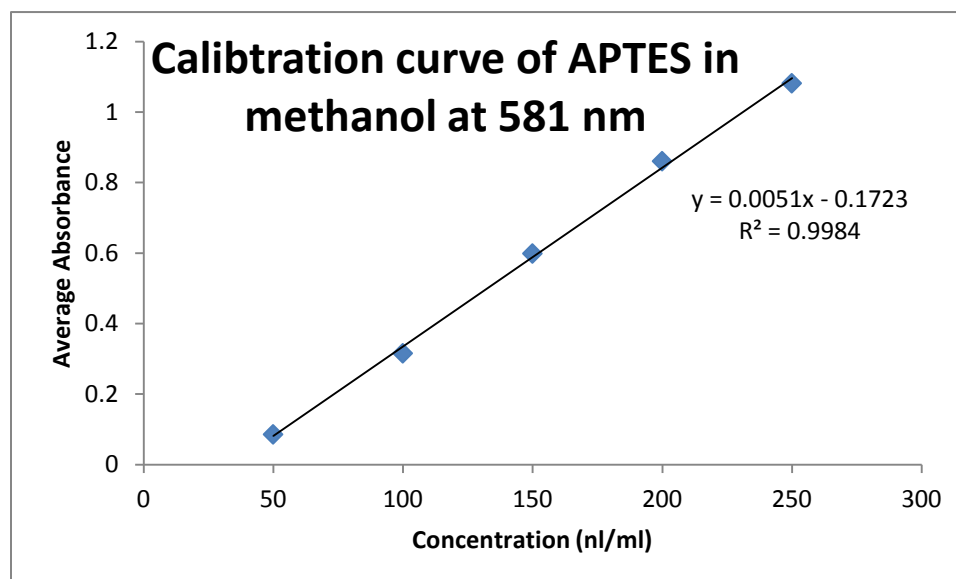


Figure 3.7: Standard calibration curve of APTES in methanol by UV Visible spectroscopy.

3.4. Estimation of folic acid conjugated to chitosan:

In the present work, folic acid (targeting moiety) has been conjugated with the pH responsive polymer (chitosan).¹⁵ Hence, in order to determine the amount of folic acid conjugated with chitosan, a calibration curve of folic acid in 0.1 N NaOH was prepared.

3.4.1. UV-Visible spectrophotometric method:

3.4.1.1. Materials:

Folic acid was purchased from Sigma Aldrich, India while sodium hydroxide pellets were purchased from Loba Chemie, India. The water used in the study was double distilled.

3.4.1.2. Equipments:

Digital Analytical Weighing Balance (Shimadzu, Switzerland)

UV-Visible Spectrophotometer 1800 (Shimadzu, Japan)

3.4.1.3. Estimation of DOX:

➤ **Reagent preparation (0.1N NaOH):**

4.0 g of sodium hydroxide was dissolved in sufficient water and volume was made up to 1000 ml with water to produce 0.1N NaOH solution.

➤ **Preparation of stock solution:**

Stock solution was prepared by dissolving 10 mg of folic acid in 100ml of 0.1N NaOH to get concentration of 100 µg/ml.

➤ **Procedure for calibration curve:**

Appropriate aliquots of stock solution of folic acid (0.5 to 2.5ml) were transferred to 10 ml volumetric flasks and made up to the mark with 0.1N NaOH to get final concentration of folic acid in range of 5-25 µg/mL. Scanning was performed in range of 800-200 nm to determine the λ_{\max} using 0.1N NaOH as blank. The absorbance maximum (λ_{\max}) was found to be 363 nm, which is the typical absorption for folic acid. The absorbance as a function of concentration for all prepared solutions was recorded against 0.1N NaOH. The procedure was repeated in triplicate and the observations were recorded. Mean value of the absorbance (n=3) along with standard deviation (S.D.) and other parameters of performed UV spectrophotometric method are recorded in table 3.8.

The regression of the plot using the method of least squares was made to evaluate the

intercept, slope and coefficient of determination (r^2) as shown in figure 3.8. The high value of r^2 (near 1) and negligible value of intercept confirmed the linearity of the calibration plot.

Table 3.8: Calibration curve of Folic acid in 0.1N NaOH by UV-Visible spectrophotometer.

Sr. No.	Concentration ($\mu\text{g/ml}$)	Mean Absorbance	\pm S.D. (n=3)
1	5	0.179	0.0019
2	10	0.305	0.0025
3	15	0.419	0.0036
4	20	0.536	0.0044
5	25	0.656	0.0049

λ_{max} (nm)	Conc. Range ($\mu\text{g/ml}$)	Mean S.D.	LOD	LOQ	Regression Equation	Regression Coefficient
363	5 - 25	0.00346	0.241	0.802	$y=0.0237x+0.064$	0.999

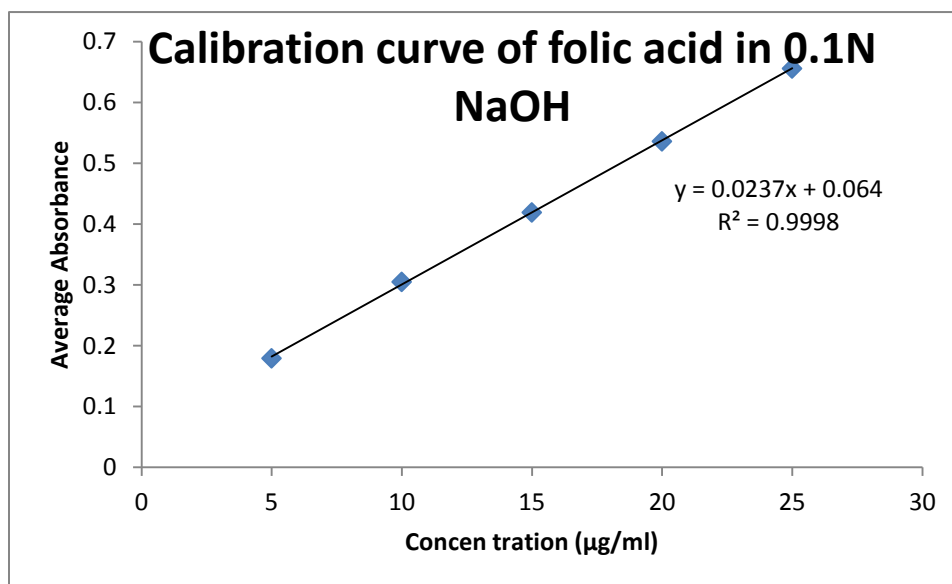


Figure 3.8: Standard calibration curve of Folic acid in 0.1N NaOH by UV Visible spectroscopy.

3.5. Lab scale method development for determination of soluble silica (silicic acid) as degradation product:

The mesoporous silica nanoparticles are known to dissolve fairly rapidly under physiological conditions when concentration levels are below the saturation level of silica. The body can absorb dissolved silica or excrete it through the urine in the form of silicic acid or oligomeric silica species.¹⁶ Here, we have developed a lab scale method for the determination of degradation of MSN by measuring silica in its soluble form (silicic acid). The developed method is capable of detecting silicic acid concentrations as low as 500 ng/mL.

3.5.1. UV-Visible spectrophotometric method:

3.5.1.1. Materials:

Sodium silicate, Ammonium molybdate, Tartaric acid and potassium ammonium tartarate were purchased from Himedia, India. Ascorbic acid was purchased from S.D. Fine Chemicals, India. Sulphuric acid was purchased from Avantor performance materials, India. Potassium dihydrogen phosphate, disodium hydrogen phosphate and sodium chloride were of analytical grade and purchased from Loba Chemie, India. All the reagents and solvents were of analytical grade. The water used in the study was double distilled.

3.5.1.2. Equipments:

Digital Analytical Weighing Balance (Shimadzu, Switzerland)

pH Meter (Labindia, India)

UV-Visible Spectrophotometer 1800 (Shimadzu, Japan)

Centrifuge (Remi, India)

3.5.1.3. Estimation of silicic acid in PBS (pH 7.4):

➤ **Reagent preparation (Phosphate buffer pH 7.4):**

2.38 g of disodium hydrogen phosphate, 0.19 g potassium dihydrogen phosphate and 8.0 g of sodium chloride were dissolved in sufficient water to produce 1000 ml and then the pH was adjusted to 7.4.

➤ **Preparation of stock solution:**

Stock solution was prepared by dissolving 47.3 mg of sodium silicate in 100ml of phosphate buffer (pH-7.4) to get concentration of 100 µg/ml of silica.

➤ **Procedure for calibration curve:**

The typical procedure involves formation of yellow silicomolybdate complex by reaction between silicic acid and ammonium molybdate in acidic conditions. Further reducing this complex using tartaric acid and reacting with Ascorbic acid yields blue colored solution whose absorbance was measured at λ_{\max} of 810 nm.

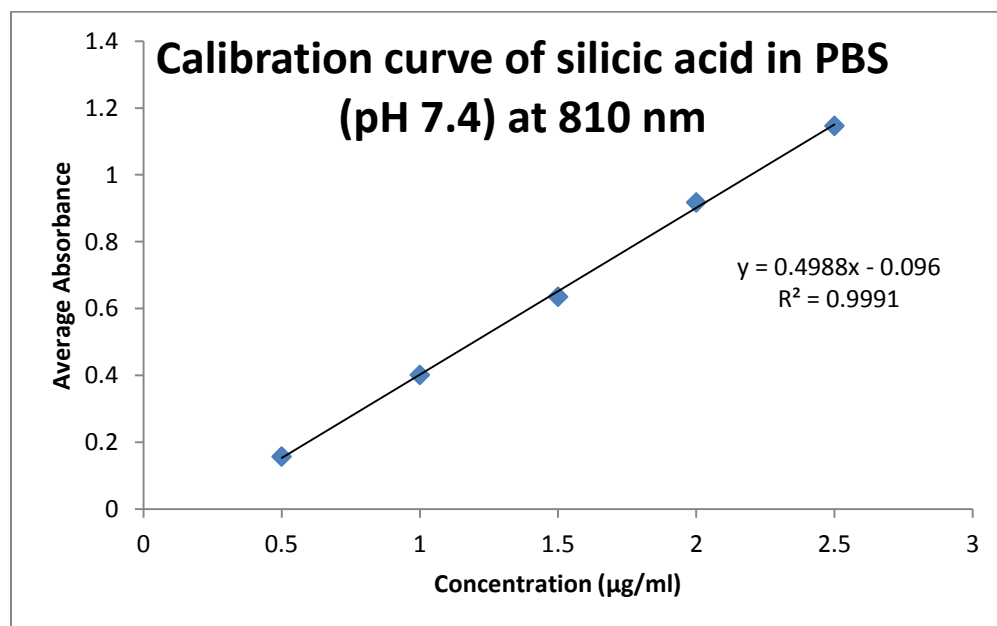
Appropriate aliquots of stock solution of sodium silicate (0.5 to 2.5ml) were transferred to 10 ml volumetric flasks and made up to the mark with phosphate buffer (pH 7.4) to get final concentration of silica in range of 5-25 $\mu\text{g/mL}$.

Now from each sample 1 ml was taken in a separate vial, to which 0.1 ml 7.5M H_2SO_4 and 1.9 ml of 10% ammonium molybdate were added. The volume was made up to 4 ml with DDW. The solution was kept aside for formation of yellow phospho molybdate (insoluble) ppt and yellow molybdosilicic acid (soluble). The molybdosilicic acid was separated by centrifugation at 5000 rpm for 5 min and filtered. 2 ml filtrate was collected for each sample and added to a separate vial which was acidified by addition of 1 ml 7.5M H_2SO_4 . 0.9 ml 10% tartaric acid solution was added to this. Immediately after tartaric acid addition, 0.1 ml potassium antimonyl tartarate (1 mg/ml) and 1 ml 1% ascorbic acid solution were added to it. The solution was kept aside for 10 minutes to develop blue coloured molybdenum blue.¹⁷ Scanning was performed in range of 900-700 nm to determine the λ_{\max} using phosphate buffer (pH 7.4) without sodium silicate (undergone above treatment) as blank. The absorbance maximum (λ_{\max}) was found to be 810 nm, which is the typical absorption for molybdenum blue. The absorbance as a function of concentration for all prepared solutions was recorded. The procedure was repeated in triplicate and the observations were recorded. Mean value of the absorbance (n=3) along with standard deviation (S.D.) and other parameters of developed UV spectrophotometric method are recorded in table 3.9. The regression of the plot using the method of least squares was made to evaluate the intercept, slope and coefficient of determination (r^2) as shown in figure 3.9. The high value of r^2 (near 1) and negligible value of intercept confirmed the linearity of the calibration plot.

Table 3.9: Calibration curve of silicic acid in PBS (pH 7.4) by UV Visible spectroscopy.

Sr. No.	Concentration ($\mu\text{g/ml}$)	Mean Absorbance	\pm S.D. (n=3)
1	0.5	0.158	0.0021
2	1.0	0.402	0.0028
3	1.5	0.636	0.0030
4	2.0	0.918	0.0039
5	2.5	1.147	0.0044

λ_{max} (nm)	Conc. Range ($\mu\text{g/ml}$)	Mean S.D.	LOD	LOQ	Regression Equation	Regression Coefficient
810	0.5 - 2.5	0.00322	0.0120	0.0400	$y=0.4988x-0.096$	0.999

**Figure 3.9:** Standard calibration curve of silicic acid in PBS (pH 7.4) by UV Visible spectroscopy.

3.5.1.4. Estimation of silicic acid in urine:

➤ **Preparation of stock solution:**

Stock solution was prepared by dissolving 4.73 mg of sodium silicate in 10ml of urine to get concentration of 100 µg/ml of silica.

➤ **Procedure for calibration curve:**

The typical procedure was similar to the procedure described in 3.5.1.3 with just one change and i.e. urine was used instead of PBS 7.4.

Table 3.10: Calibration curve of silicic acid in urine by UV Visible spectroscopy.

Sr. No.	Concentration (µg/ml)	Mean Absorbance	± S.D. (n=3)
1	0.5	0.162	0.0018
2	1.0	0.321	0.0025
3	1.5	0.467	0.0029
4	2.0	0.626	0.0039
5	2.5	0.748	0.0046

λ_{\max} (nm)	Conc. Range (µg/ml)	Mean S.D.	LOD	LOQ	Regression Equation	Regression Coefficient
810	0.5 - 2.5	0.00314	0.0183	0.0609	$Y=0.2954x+0.0217$	0.998

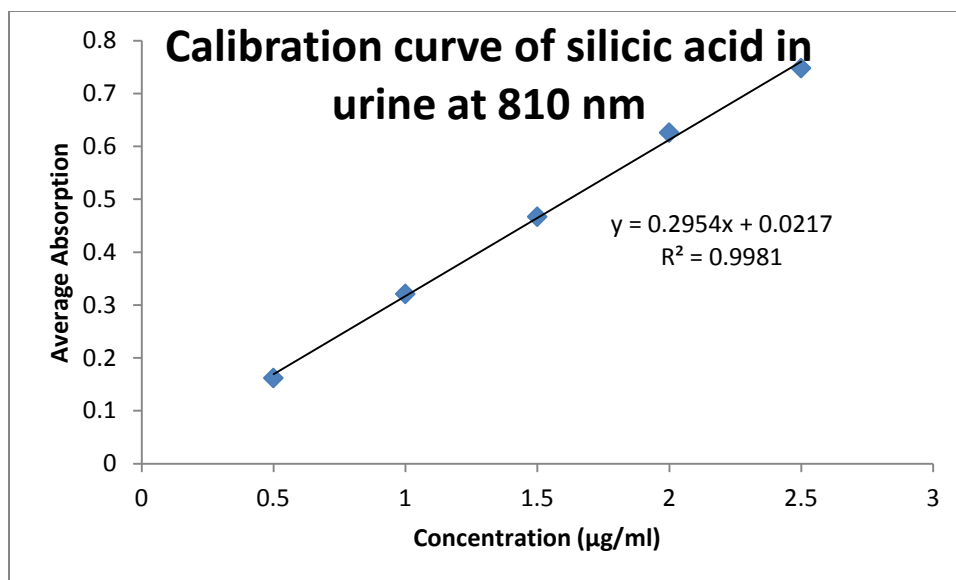


Figure 3.10: Standard calibration curve of silicic acid in urine by UV Visible spectroscopy.

References:

1. Wang Y, Luo Q, Sun R, Zha G, Li X, Shen Z, Zhu W. Acid-triggered drug release from micelles based on amphiphilic oligo(ethylene glycol)-doxorubicin alternative copolymer. *Journal of Materials Chemistry B*. 2014, 2:7612-7619.
2. Kumari M, Agrawal A, Mishra TS, Kumari M, Bhawarker S. Quantitative estimation of dextran conjugated PPI dendrimer for delivery of doxorubicin hydrochloride as an anticancer drug. *World Journal Of Pharmacy and Pharmaceutical Sciences*. 2017, 6(4):1260-1273.
3. Panda P, Taviti AC, Satpati S, Kar MM, Dixit A, Beuria TK, Doxorubicin inhibits E. coli division by interacting at a novel site in FtsZ. *Biochemical Journal*. 2015, 471:335-346.
4. Maltas E, Gubbuk IH, Yildiz S. Development of doxorubicin loading platform based albumin-sporopollenin as drug carrier. *Biochemistry and Biophysics Reports*. 2016, 7:201-205.
5. Beaty RD, Kerber JD. *Concepts, Instrumentation and Techniques in Atomic Absorption Spectrophotometry*. The Perkin-Elmer Corporation, second edition, 1993:1-3.
6. Walsh A. The application of atomic absorption spectra to chemical analysis. *Spectrochimica Acta*. 1955, 7:108-117.
7. Russell BJ, Shelton JP, Walsh A. An atomic-absorption spectrophotometer and its application to the analysis of solutions. *Spectrochimica Acta*. 1957, 8:319-328.
8. Allan JE. Atomic-absorption spectrophotometry with special reference to the determination of magnesium. *Analyst*. 1958, 83:466-471.
9. David DJ. Determination of zinc and other elements in plants by atomic-absorption spectroscopy. *Analyst*. 1958, 83:655-661.
10. Allan JE. The determination of iron and manganese by atomic absorption. *Spectrochimica Acta*. 1959, 15:800-806.
11. Allan JE. The determination of copper by atomic absorption spectrophotometry. *Spectrochimica Acta*. 1961, 17:459-466.
12. Zhang J, Niemela M, Westermarck J, Rosenholm J. Mesoporous silica nanoparticles with redox-responsive surface linkers for charge-reversible loading and release of short oligonucleotides. *Dalton Transactions*. 2014, 43(10):4115-4126.

13. Lu HT. Synthesis and Characterization of Amino-Functionalized Silica Nanoparticles. *Colloid Journal*. 2013, 75(3): 311-318.
14. Hung BY, Kuthati Y, Kankala RK, Kankala S, Deng JP, Liu CL, Lee CH. Utilization of Enzyme-Immobilized Mesoporous Silica Nanocontainers (IBN-4) in Prodrug-Activated Cancer Theranostics. *Nanomaterials*. 2015, 5:2169-2191.
15. Daryasari MP, Akhgar MR, Mamashli F, Bigdeli B, Khoobi M. Chitosan-folate coated mesoporous silica nanoparticles as a smart and pH-sensitive system for curcumin delivery. *RSC Advances*. 2016, 6:105578-105588.
16. Rosenholm J, Mamaeva V, Sahlgren C, Linden M. Nanoparticles in targeted cancer therapy: Mesoporous silica nanoparticles entering preclinical development stage. *Nanomedicine*. 2012, 7(1):111-120.
17. Ramachandran R, Gupta PK. An improved spectrophotometric determination of silicate in water based on molybdenum blue. *Analytica Chimica Acta*. 1985, 172:307-311.